



Photonic generation of a microwave waveform with an ultra-long temporal duration using a frequency-shifting dispersive loop

RUIDONG CAO,¹ GUANGYING WANG,¹ MINGHAI LI,¹ JIEJUN ZHANG,^{1,*}  AND JIANPING YAO² 

¹Guangdong Provincial Key Laboratory of Optical Fiber Sensing and Communications, Institute of Photonics Technology, Jinan University, Guangzhou 511443, China

²Microwave Photonics Research Laboratory, School of Electrical Engineering and Computer Science, University of Ottawa, Ottawa, ON K1N 6N5, Canada

*zhangjiejun@jnu.edu.cn

Abstract: A photonic approach to generate a linearly chirped microwave waveform (LCMW) with an ultra-long temporal duration is proposed and experimentally demonstrated. The microwave waveform generation is achieved based on spectral-shaping and wavelength-to-time (SS-WTT) mapping by using a Mach-Zehnder interferometer (MZI) and a frequency-shifting dispersive loop (FSDL), respectively. To make the generated microwave waveform have an ultra-long temporal duration, the FSDL is operating to allow a spectrally shaped optical pulse to recirculate in a dispersive loop multiple times with a low propagating loss, to generate a microwave waveform with a temporal duration that is more than one order of magnitude longer than that of a microwave waveform generated using a dispersive element without recirculation. To generate a LCMW, the spectral shaper is configured to have a free spectral range (FSR) that is linearly increasing or decreasing with optical wavelength. The proposed approach is experimentally demonstrated. Two LCMWs, by allowing an optical pulse recirculating in the FSDL for three and seven round trips, tripled and septupled temporal durations of 64 and 182 ns are generated. The generation of two LCMWs with ultra-long temporal durations of 370 ns and 450 ns are also demonstrated.

© 2022 Optica Publishing Group under the terms of the [Optica Open Access Publishing Agreement](#)

1. Introduction

Microwave waveform with a large time-bandwidth product (TBWP) can find applications, such as radar, spread spectrum communications, aerial photography, and modern instrumentation. In a radar system, for example, a linearly chirped microwave waveform (LCMW) with a long temporal duration and wide bandwidth is needed for long range and high-resolution measurement [1,2]. An LCMW with a long temporal duration can be generated electronically, but the bandwidth and central frequency are often limited to a few gigahertz due to the electronic bandwidth bottleneck. In a modern high-resolution microwave imaging system, an LCMW with a bandwidth and a central frequency up to tens or even hundreds of gigahertz is required, which is a great challenge using electronic techniques.

For the past decades, photonic generation of broadband LCMWs has been studied extensively thanks to the large bandwidth offered by modern photonics [3,4]. Numerous solutions have been proposed, including LCMW generation based on direct space-to-time pulse shaping (DST) [5–7], temporal pulse shaping (TPS) [8,9], microwave photonic filtering (MPF) [10,11], optical heterodyne [12], optoelectronic oscillation [13–16], and spectral-shaping and wavelength-to-time (SS-WTT) mapping [17–21]. The two approaches based on optoelectronic oscillation and SS-WTT mapping are most widely studied due to their flexibility and simplicity for broadband and high-quality LCMW generation. In [13], an LCMW was generated by applying quadratic phase modulation to a microwave signal generated by an optoelectronic oscillator (OEO). However, a

high-voltage modulation waveform is needed, and the generated LCMW only still has a short temporal duration of about 0.5 ns. To generate an LCMW with a long temporal duration, a Fourier domain mode-locked (FDML) OEO can be employed [15,16]. To achieve Fourier domain mode locking, a frequency-tunable microwave bandpass filter (MBPF) should be incorporated in the OEO loop, which can be implemented using a purely electronic microwave bandpass filter, but with limited frequency tunable range and slow tuning speed or a microwave photonic bandpass filter with a much wider tunable range and higher tuning speed. By applying a frequency tunable signal with a period equal to the round-trip time of the OEO to the microwave bandpass filter, Fourier domain mode locking can be realized and an LCMW with a broad bandwidth and long temporal duration can be generated [15,16,22]. However, to achieve accurate Fourier domain mode locking, the microwave bandpass filter must have a very small bandwidth of a few or tens of kHz to select only a single mode at a time, which is hard to implement. A microwave bandpass filter with a central frequency at the GHz band usually has a bandwidth of a few MHz. With the use of such a microwave bandpass filter, multiple modes are selected at one time, making the selected modes in the passband not phase locked, and thus the generated LCMW has poor phase noise performance.

An LCMW with a broad bandwidth and high frequency can also be generated based on SS-WTT mapping. In an SS-WTT mapping system, an ultra-short optical pulse is spectrally shaped by a spectral shaper, which can be an optical filter, and the shaped spectrum is mapped to the time domain by a dispersive element. By applying the time-domain optical signal to a photodetector (PD), a microwave waveform is generated. To generate an LCMW, the optical filter (as a spectral shaper) should have a spectral response with a free spectral range (FSR) that is linearly increasing or decreasing with wavelength. Such a filter can be an optical interferometer, such as a Mach-Zehnder interferometer (MZI) with a wavelength dependent arm length or a Sagnac interferometer with a wavelength dependent loop length [17–21]. The temporal duration of a generated LCMW is dependent on the value of dispersion of the dispersive element used to perform WTT mapping. Due to the limited dispersion, an LCMW generated based on SS-WTT mapping has a short temporal duration, usually less than a few nanoseconds. To increase the effective value of dispersion, a recirculating fiber-optic dispersive loop was employed, to allow a spectrally shaped pulse to recirculate in the loop multiple times [21]. To avoid power reduction of the pulse in the loop, an optical amplifier was incorporated. However, the gain of the optical amplifier cannot be too high, since the net loop gain must be controlled smaller than unity to avoid optical oscillation, the pulse after only a few rounds of recirculation becomes weak with poor signal to noise ratio (SNR), making the number of recirculation limited. In the demonstration reported in [21], the temporal duration of a generated LCMW was only 42 ns. The same approach to extend the pulse duration based on a recirculating loop was also reported in [23]. Again, due to the limited number of recirculation, the temporal duration of the generated LCMWs is limited.

In this paper, we propose and experimentally demonstrate a novel approach to generate an LCMW with a significantly extended temporal duration based on SS-WTT mapping using a frequency-shifting dispersive loop (FSDL) with large equivalent dispersion. Since the frequency of the optical pulse is shifted after each recirculation, optical oscillation is effectively avoided. By using an optical amplifier with a high gain to compensate for the loop loss, a spectrum-shaped optical pulse can travel in the recirculating loop more times than using a simple dispersive loop without frequency shifting, leading to the generation of an LCMW with significantly extended temporal duration. In the proposed system, the spectral shaper is realized using an MZI incorporating a dispersive fiber in one arm to produce a wavelength-dependent FSR. An ultra-short pulse generated by a mode-locked laser (MLL) is sent to the spectral shaper, and the spectrally shaped optical pulse is forwarded to the FSDL to perform WTT mapping. In the FSDL, an acoustic-optic modulator (AOM) is incorporated to shift the optical frequency of the spectrum-shaped pulse after each recirculation, to effectively eliminate optical oscillation

although the gain of an optical amplifier can be controlled high, to allow the pulse to travel in the recirculating loop more times. The proposed approach is evaluated experimentally. Two LCMWs with temporal durations of 64 and 182 ns by allowing an optical pulse recirculating in the FSDL for 3 and 7 round trips having tripled and septupled temporal durations are generated. The generation of two LCMWs with ultra-long temporal duration of 370 ns and 450 ns are also demonstrated.

2. Principle

Figure 1(a) illustrates the schematic diagram of the proposed LCMW generation system based on SS-WTT mapping using an MZI and an FSDL. An ultra-short optical pulse train is generated by an MLL and is sent to a dispersion compensating fiber (DCF1) to lower the peak power to avoid the damage of the optical components. To avoid overlapping of adjacent optical pulses when recirculating in the FSDL, the repetition rate is reduced by using a Mach-Zehnder modulator (MZM) as an optical switch which is controlled by a switching signal from an arbitrary waveform generator (AWG) [24]. A polarization controller (PC1) is employed between DCF1 and the MZM to minimize the polarization-dependent loss in the MZM. The repetition-rate-reduced pulse train is sent to the spectral shaper which is an MZI formed by two optical couplers (OC1 and OC2) with the upper arm having a dispersion compensating fiber (DCF2) and a tunable delay line (TDL) and the lower arm a PC (PC2) [25], as shown in Fig. 1(b). Due to the dispersion-dependent time delay of DCF2, the spectral shaper has a linearly increasing or decreasing FSR with wavelength. The length difference between the two arms can be tuned by tuning the TDL and the polarization states between the two arms can be aligned by tuning PC2 to achieve an interference spectrum with the highest visibility.

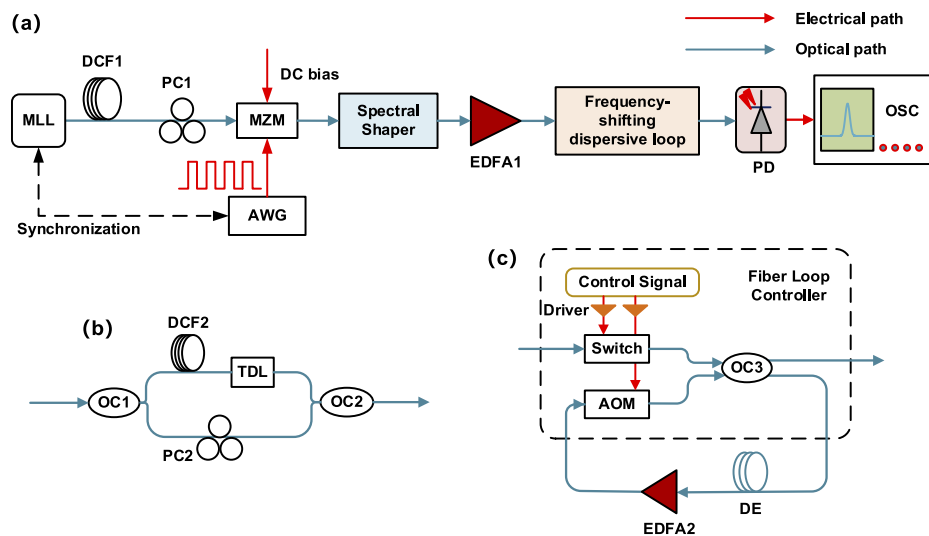


Fig. 1. (a) Schematic diagram of the proposed microwave waveform generation system; (b) the spectral shaper and (c) the frequency-shifting dispersive loop. MLL: mode-locked laser; DCF: dispersion compensating fiber; PC: polarization controller; AWG: arbitrary waveform generator; FLC: fiber loop controller; TDL: tunable delay line; OC: optical coupler; EDFA: erbium-doped fiber amplifier; DE: dispersive element; AOM: acousto-optic modulator; PD: photodetector; OSC: oscilloscope.

The optical signal from the spectral shaper is then amplified by an erbium-doped fiber amplifier (EDFA1) and sent to the FSDL to perform WTT mapping. As shown in Fig. 1(c), the FSDL consists of a fiber loop controller (FLC) in which an optical switch and an AOM are synchronized

to control the number of round trips that an optical pulse can recirculate in the loop. A dispersive element (DE) and an EDFA (EDFA2) are incorporated in the FLC to provide, respectively, dispersion and gain. In addition, since the optical wavelength of the optical pulse is shifted after passing through the AOM on a round-trip basis, the gain of EDFA2 can be controlled large to fully compensate for the round-trip loss, to maximize the number of round trips that an optical pulse can recirculate in the loop [21]. A dispersed pulse (after WTT mapping) is coupled out of the loop via a third OC (OC3) and is detected at the PD to generate an LCMW. The output waveform is monitored by an oscilloscope (OSC).

In the following, an analysis is performed to show the relationship between the number of round trips and the instantaneous frequency of a generated LCMW. In the analytical study, we ignore the dispersion of DCF1 as it is small and has negligible effect as compared to the FSDL with much greater dispersion, and the gain and loss of all components are not considered. Ideally, an optical pulse from an MLL has a Gaussian spectral shape, which is given by

$$G(\omega) = \exp \left[- \left(\frac{\omega - \omega_0}{\omega_B} \right)^2 \right] \quad (1)$$

where ω is the optical angular frequency, ω_0 and ω_B are the center frequency and bandwidth of the optical pulses, respectively. The optical pulse is sent to the spectral shaper, which is an MZI with the length difference between the two arms L given by

$$L(\omega) = \Delta L - [\Phi_1(\omega - \omega_0) + \tau] \left(\frac{c}{n_{\text{eff}}} \right) \quad (2)$$

where ΔL is the fixed physical length difference between the two arms with respect to the reference optical frequency ω_0 , Φ_1 is the dispersion coefficient of DCF2, c is the light velocity in vacuum, n_{eff} is the effective refractive index of the fiber, and τ is a tunable time delay introduced by the TD. As can be seen, the length difference between the two arms of the MZI is frequency dependent. The FSR of the MZI is given by

$$\begin{aligned} FSR(\omega) &= \frac{2\pi c}{n_{\text{eff}} L(\omega)} \\ &= \frac{2\pi c}{n_{\text{eff}} \Delta L - c[\Phi_1(\omega - \omega_0) + \tau]} \end{aligned} \quad (3)$$

which is also frequency dependent. The spectral response of the MZI has a shape that is described by a sinusoidal function with an increasing period (or FSR) given by [21,25]

$$\begin{aligned} H(\omega) &= \sin \left(\frac{2\pi}{FSR_\omega} \omega + \varphi_0 \right) \\ &= \sin \left[\left(\frac{n_{\text{eff}} \Delta L}{c} + \Phi_1 \omega_0 - \tau \right) \omega - \Phi_1 \omega^2 + \varphi_0 \right] \end{aligned} \quad (4)$$

where φ_0 is an initial phase. After spectral shaping, at the output of the MZI, the spectrum of the optical pulse is given by

$$\begin{aligned} Y(\omega) &= G(\omega) \times H(\omega) \\ &= G(\omega) \times \sin \left[\left(\frac{n_{\text{eff}} \Delta L}{c} + \Phi_1 \omega_0 - \tau \right) \omega - \Phi_1 \omega^2 + \varphi_0 \right] \end{aligned} \quad (5)$$

Then, the optical pulse is launched into the FSDL for WTT mapping. The equivalent dispersion coefficient of the loop is $N\Phi_2$, where N is the number of round trips that the optical pulse travels

in the dispersive loop and Φ_2 is the dispersive coefficient of the DE. The optical signal from the dispersive loop after WTT mapping is given by [4]

$$y(t) \approx \exp\left(j\frac{1}{2N\Phi_2}t^2\right) \times Y(\omega) \Bigg|_{\omega=\frac{t}{N\Phi_2}} \tag{6}$$

where the exponential term is the impulse response of the FSDL with an equivalent dispersion coefficient of $N\Phi_2$. After optical-electrical conversion at the PD, an electrical waveform is generated which is given by

$$\begin{aligned} i_{PD}(t) &= \Re \times [y(t) \times y(t)^*] \\ &= \Re \left| \exp\left(j\frac{1}{2N\Phi_2}t^2\right) \times Y_2(\omega) \Big|_{\omega=\frac{t}{N\Phi_2}} \right|^2 \\ &= \frac{\Re}{2} |G(\omega)|^2 \times \left[1 - \cos\left(\frac{2n_{\text{eff}}\Delta L t}{cN\Phi_2} + \frac{2(\Phi_1\omega_0 - \tau)t}{N\Phi_2} - \frac{2\Phi_1 t^2}{N^2\Phi_2^2} + 2\varphi_0\right) \right] \end{aligned} \tag{7}$$

where \Re is responsivity of the PD, $i_{PD}(t)$ is the current of the generated LCMW. The instantaneous frequency of the LCMW is given by

$$\begin{aligned} f &= \frac{1}{2\pi} \frac{d}{dt} \left(\frac{2n_{\text{eff}}\Delta L t}{cN\Phi_2} + \frac{2(\Phi_1\omega_0 - \tau)t}{N\Phi_2} - \frac{2\Phi_1 t^2}{N^2\Phi_2^2} + 2\varphi_0 \right) \\ &= \frac{1}{2\pi} \left(\frac{2n_{\text{eff}}\Delta L}{cN\Phi_2} + \frac{2(\Phi_1\omega_0 - \tau)}{N\Phi_2} - \frac{4\Phi_1}{N^2\Phi_2^2} t \right) \\ &= \frac{n_{\text{eff}}\Delta L + c(\Phi_1\omega_0 - \tau)}{\pi cN\Phi_2} - \frac{2\Phi_1}{\pi N^2\Phi_2^2} t. \end{aligned} \tag{8}$$

As can be seen, when the dispersion coefficients Φ_1 and Φ_2 are given, the central frequency of the LCMW is dependent on the time delay τ introduced by the TDL and the number of round trips N . In general, the central frequency tunable range is decreased as the number of round trips is increased. If a large central frequency tunable range is needed, a TDL with a larger tuning range should be used.

The temporal duration of the LCWM is given by [4,21]

$$T = N\Phi_2 \times \omega_B \tag{9}$$

As can be seen, the temporal duration of the LCMW is proportional to the number of round trips of a spectrally shaped optical pulse recirculating in the dispersive loop.

Based on Eqs. (5) and (8), we calculate the spectrum of the optical signal at the output of the spectral shaper, which is shown in Fig. 2(a). The LCMWs generated by the system when the optical pulse recirculates in the dispersive loop for one, three and seven round trips are shown in Fig. 2(b), 2(c) and 2(d), respectively. As can be seen, the spectrum of the optical pulse at the output of the spectral shaper is mapped to the time domain, resulting in the generation of a chirped microwave waveform with a linearly varying instantaneous frequency. The central frequency and the chirp rate of the generated waveform can be tuned by changing the time delay introduced by the TDL and the dispersion coefficient of DCF2, respectively. On the other hand, the temporal duration of the generated waveform can be increased by increasing the number of round trips to have large effective dispersion to implement WTT mapping by recirculating the optical pulse in the dispersive loop for more round trips.

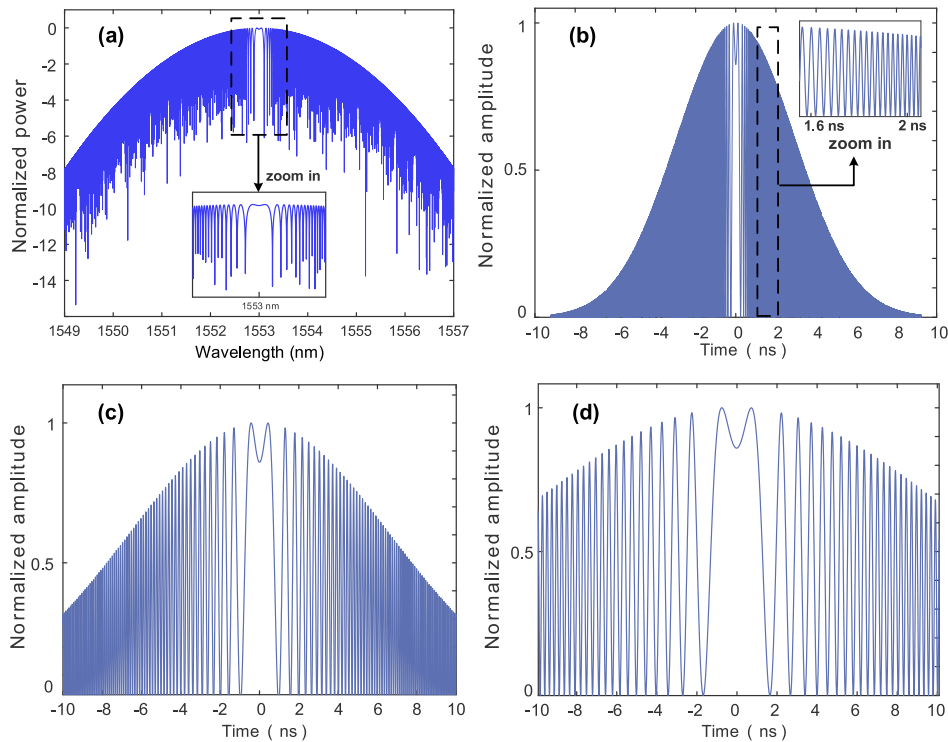


Fig. 2. (a) Calculated spectrum of the spectrally shaped optical pulse. Calculated LCMWs at the output of the PD after the optical pulse recirculates in the FSDL for (b) one, (c) three and (d) seven round trips in the FSDL.

3. Experiment

An experiment is performed based on the setup shown in Fig. 1 to evaluate the effectiveness of the proposed approach for LCMW generation with an increased temporal duration. An ultra-short optical pulse train generated by an MLL (Calmar Laser FPL-03CFF) with a repetition rate of 20 MHz is sent to the MZM through PC1, to have its repetition rate reduced to 50 kHz, to avoid overlapping between adjacent optical pulses. The MZM is biased at its minimum transmission point and is driven by a gate signal from an AWG with a frequency of 50 kHz and an open window of 50 ns. The pulse train is dispersed by DCF1 with a dispersion coefficient of 1269 ps^2 to reduce the peak power. The pulse train after DCF1 is sent to the spectral shaper, in which the dispersion coefficient of DCF2 is 168 ps^2 . Figure 3 shows the spectrum of the pulse train at the output of the spectral shaper, measured by an optical spectrum analyzer (OSA). A wavelength-dependent FSR can be seen, which agrees with the theoretical prediction given by Eq. (3). The two arms of the MZI have a matched optical length at 1553.3 nm, where the interference spectrum has the largest FSR. Due to the limited spectral resolution of 0.02 nm of the OSA, the interference spectrum, cannot be seen at wavelengths about 2 nm away from the central wavelength of 1553.3 nm. Note that the spectrum of the pulse generated by the MLL we use has ripples up to 2 dB within its 3-dB spectral bandwidth. To show the interference spectrum more clearly, the optical spectrum in Fig. 3 is calibrated using the directly measured MLL spectrum to eliminate the ripples. The spectrally shaped pulse train is sent to the FSDL in which the repetition rate is further reduced to 25 kHz (or a period of 40 μs) by the FLC by applying a rectangular waveform with a repetition rate of 25 kHz to control the switch in the FLC. The DE in the FSDL has a dispersion coefficient of 1683 ps^2 . After WTT mapping, the

spectrally shaped pulse is converted to a temporal pulse with a shape identical to the spectrum of the shaped pulse and a microwave waveform is generated. The generated microwave waveform is monitored by a real-time oscilloscope (Tektronix DSA72004B).

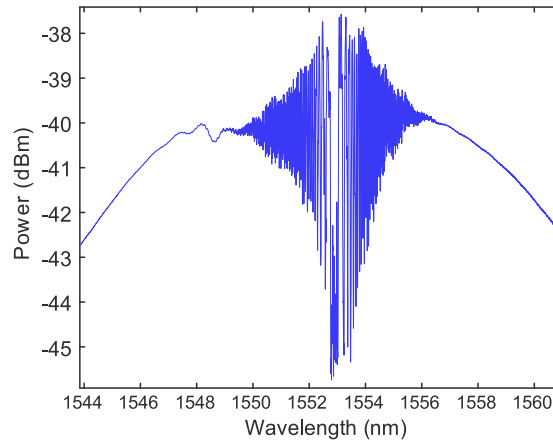


Fig. 3. Measured spectrum of the spectrally shaped optical pulse at the output of the spectral shaper.

Figure 4 shows the generated microwave waveforms when an optical pulse is launched into the FSDL and is recirculating in the FSDL up to 20 round trips. As can be seen, due to the recirculation of the input optical pulse in the FSDL, a single optical pulse is converted to a pulse burst of 20 individual pulses. The time interval between two adjacent pulses is around $1.92 \mu\text{s}$, corresponding to the physical length of the loop of around 400 m. By configuring the FLC, the pulses after recirculating for more than 20 round times are blocked by the FLC to avoid overlapping with the next pulse burst. For an input pulse train with a lower repetition rate, the maximum number of round trips can be further increased to generate microwave waveforms with longer temporal durations.

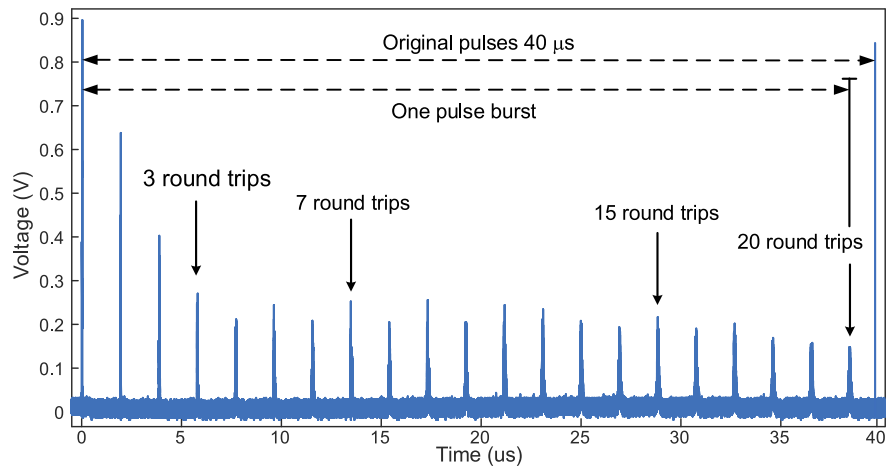


Fig. 4. Measured microwave pulse burst at the output of the PD as an optical pulse is launched and recirculates in the FSDL.

Figure 5 shows the zoom-in views of the microwave waveforms after recirculating in the FSDL for three and seven round trips. The shapes of the waveforms resemble the spectrum of the

spectrally shaped pulse, thanks to the linear WTT mapping process. Due to the wavelength-dependent FSR of the spectral shaper, the microwave waveforms are linearly chirped with a down-chirp portion and an up-chirp portion. The temporal durations of the waveforms after three and seven round trips are 64 and 182 ns, respectively, which are three and seven times that of the microwave waveform without recirculation. Due to the Gaussian spectrum of an optical pulse generated by the MLL, the LCMWs shown in Fig. 5(a) and 5(b) have a Gaussian envelope. In addition, the envelopes have fluctuations, especially at high frequencies, which are caused by the uneven gain spectrum of EDFA2 and the frequency-dependent responsivity of the PD and the sampling system. One key feature of using an LCMW is the ability for pulse compression. Figure 5(c) and 5(d) shows the calculated autocorrelations of the LCMWs when the spectrally shaped pulse is recirculating in the FSDL for three and seven round trips. Clearly, the waveforms are significantly compressed.

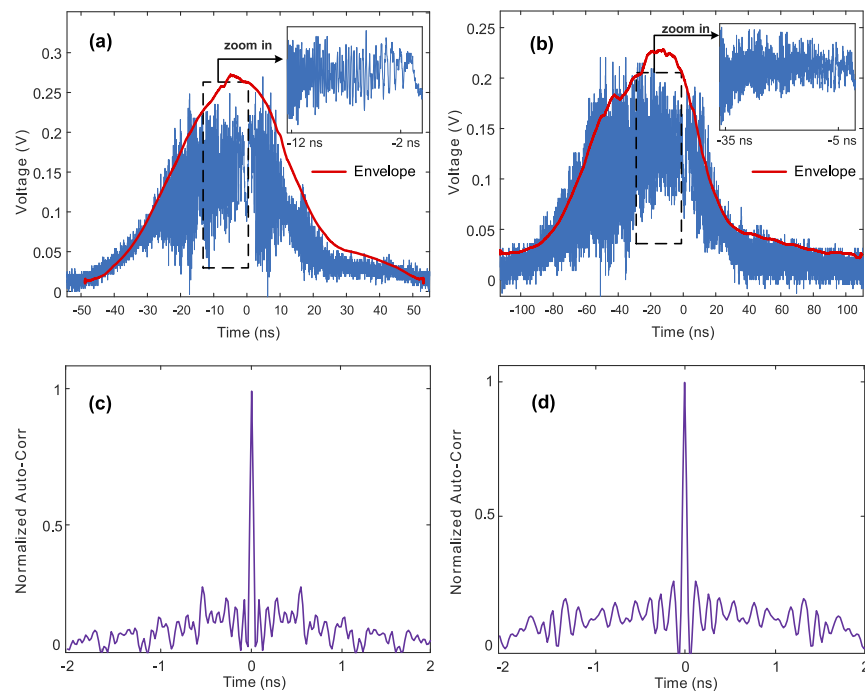


Fig. 5. Generated LCMWs when a spectrally shaped pulse is recirculating in the FSDL for (a) three and (b) seven round trips. The calculated autocorrelations of the LCMWs when the spectrally shaped pulse is recirculating in the FSDL for (c) three and (c) seven round trips.

To have more details about the generated LCMWs, we calculate the spectrograms of the generated LCMWs with the numbers of round trips of three and seven. Figure 6(a) and 6(b) shows the spectrograms of the waveforms in Fig. 5(a) and 5(b). A good linearity between instantaneous frequency and time can be observed. Figure 6(c) and 6(d) shows the simulated spectrograms of the LCMWs after three and seven round trips. A slight disagreement between the spectrograms in Fig. 6(a) and 6(c) is observed, which is caused due to the limited bandwidths of the PD and the oscilloscope, which are 20 and 25 GHz, respectively. Therefore, the part of the waveforms with instantaneous frequencies beyond 20 GHz cannot be correctly detected and sampled in the experiment. This problem will disappear if the number of round trips is increased, since the higher the number of round trips, the wider the temporal duration of a generated LCMW, and the lower the instantaneous frequency and bandwidth. This conclusion is confirmed by the

spectrograms in Fig. 6(b) and 6(d), where the number of round trips is increased to seven. A good agreement between the experimental and simulated spectrograms is clearly observed.

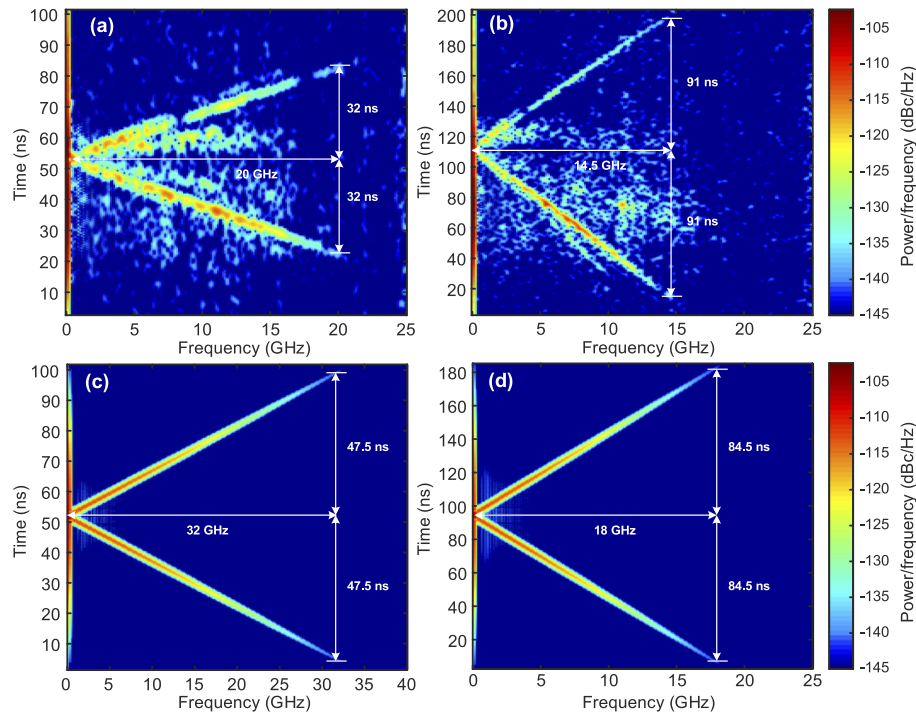


Fig. 6. Spectrograms of the generated LCMWs for (a) three and (b) seven round trips in Fig. 5. Simulated spectrogram results for (c) three and (d) seven round trips.

Note also that the generated LCMWs shown in Fig. 5(a) and 5(b) and the spectrograms shown in Fig. 6(a) and 6(b) are noisy due to the additional noise introduced by EDFA2. To mitigate the signal-to-noise ratio (SNR) degradation, accurate power management should be adopted in the loop to ensure EDFA2 is operating at an optimum input power level.

Theoretically, an optical pulse recirculating in a dispersive loop does not increase the TBWP of the generated waveform, since the factor of temporal stretching is the same as that of the bandwidth compression. However, for a waveform generation system with a given bandwidth, due to the bandwidth reduction in the generated microwave waveform, the spectrum of a time stretched waveform can pass the waveform generation system with less attenuation, thus making the TBWP increased. For the system implemented in the experiment, the bandwidth is limited by the PD, which is 20 GHz. For the LCMWs after three and seven round trips, the bandwidths are 40 and 29 GHz. Clearly, the spectrum of the microwave waveform after three round trips is filtered more than the microwave waveform after seven round trips, which would make the TBWPs of the two microwave waveforms reduced, but the one with three round trips has more reduction in TBWP. In the experiment, the TBWPs of the LCMWs after three and seven round trips are measured to be 2560 and 5278, respectively. The theoretical TBWPs of the two microwave waveforms without considering the limited bandwidth of the system should be 6080.

To evaluate the temporal stretching with more round trips, we also measure the microwave waveforms after 15 and 20 round trips. Figure 7 shows the spectrograms of the microwave waveforms for 15 and 20 round trips in which the gain ripples of the EDFA is flattened digitally. Thanks to the reduction in bandwidth, the temporal durations of the LCMWs are measured to be 370 ns and 450 ns, respectively, which are larger than those of the microwave waveforms after

three and seven round trips. The TBWP of the LCMW after 15 round trips should be comparable to that measure in Fig. 6(b) of around 5278, and the temporal duration of the LCMW after 20 round trips can be as long as 450 ns, which can be further increased to a few microseconds with a larger number of round trips. Nevertheless, the LCMW with a temporal duration of 450 ns in Fig. 7(b) is longer than those in Fig. 6, and it is the longest ever reported for microwave waveforms generation based on SS-WTT mapping. In fact, it is more than one order of magnitude longer than a microwave waveform generated using a dispersive element without recirculation.

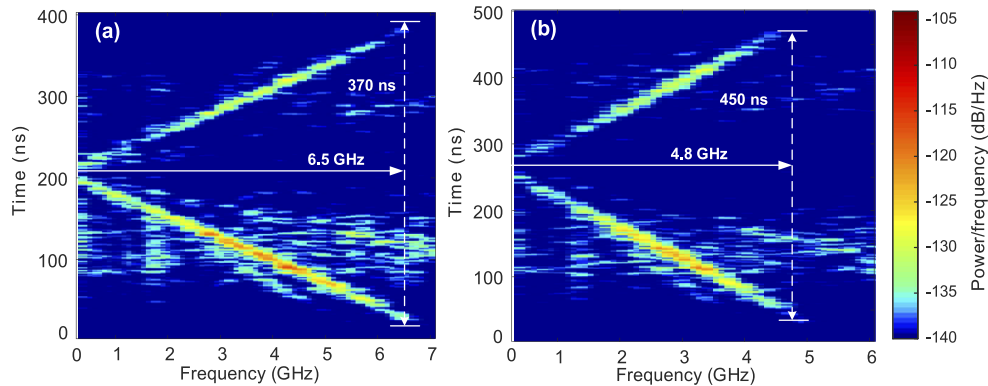


Fig. 7. Spectrograms of the generated LCMWs for (a) 15 and (b) 20 round trips.

4. Conclusion

A novel approach to generate LCMWs based on SS-WTT mapping with a long temporal duration using an MZI and an FSDL, respectively, was proposed and experimentally demonstrated. In the proposed system, the spectral shaping was implemented by an MZI incorporating a DCF and an TDL in one arm to achieve a wavelength-dependent and tunable FSR. The WTT mapping was realized using an FSDL, which was formed using an AOM, a DE and an EDFA. Since the frequency of the optical pulse recirculating in the FSDL was shifted by the AOM after each recirculation, optical oscillation was fully eliminated, making it possible to allow the EDFA to have a higher gain to fully compensate for the loop loss. The proposed system was evaluated experimentally. Two LCMWs with an optical pulse recirculating in the FSDL for three and seven round trips having tripled and septupled temporal durations of 64 and 182 ns were generated. The generation of two LCMWs with ultra-long temporal duration of 370 and 450 ns were also demonstrated. To further improve the quality of the generated LCMW, active spectrum and optical power control may be used in the system to compensate for the uneven mode-locked laser spectrum and the EDFA gain spectrum, thus allowing the generation of an LCMW with a flatter envelope and with an improved SNR, and further increasing the maximum allowable number of round trips to achieve a longer temporal duration. The work provided a solution to effectively increase the temporal duration of a microwave waveform.

Funding. Guangdong Province Key Field R&D Program Project (2020B0101110002); National Natural Science Foundation of China (61860206002, 61905095, 62101214).

Disclosures. The authors declare no conflicts of interest.

Data availability. Data underlying the results presented in this paper are not publicly available at this time but may be obtained from the authors upon reasonable request.

References

1. M. A. Richards, J. Scheer, W. A. Holm, and W. L. Melvin, *Principles of modern radar* (Citeseer, 2010).

2. D. K. Barton, *Radar System Analysis and Modeling* (Artech House, 2004).
3. J. Yao, "Microwave Photonics," *J. Lightwave Technol.* **27**(3), 314–335 (2009).
4. J. Yao, "Photonic generation of microwave arbitrary waveforms," *Opt. Commun.* **284**(15), 3723–3736 (2011).
5. D. E. Leaird and A. J. O. L. Weiner, "Chirp control in the direct space-to-time pulse shaper," *Opt. Lett.* **25**(11), 850–852 (2000).
6. J. D. McKinney, S. Dongsun, D. E. Leaird, and A. M. Weiner, "Photonic assisted generation of arbitrary millimeter-wave and microwave electromagnetic waveforms via direct space-to-time optical pulse shaping," *J. Lightwave Technol.* **21**(12), 3020–3028 (2003).
7. A. Vega, D. E. Leaird, and A. M. J. O. L. Weiner, "High-speed direct space-to-time pulse shaping with 1 ns reconfiguration," *Opt. Lett.* **35**(10), 1554–1556 (2010).
8. C. Wang, M. Li, and J. Yao, "Continuously tunable photonic microwave frequency multiplication by use of an unbalanced temporal pulse shaping system," *IEEE Photonics Technol. Lett.* **22**(17), 1285–1287 (2010).
9. M. Li, C. Wang, W. Li, and J. Yao, "An unbalanced temporal pulse-shaping system for chirped microwave waveform generation," *IEEE Trans. Microwave Theory Tech.* **58**(11), 2968–2975 (2010).
10. C. Wang and J. Yao, "Chirped microwave pulse compression using a photonic microwave filter with a nonlinear phase response," *IEEE Trans. Microwave Theory Tech.* **57**(2), 496–504 (2009).
11. Y. Dai and J. Yao, "Chirped microwave pulse generation using a photonic microwave delay-line filter with a quadratic phase response," *IEEE Photonics Technol. Lett.* **21**(9), 569–571 (2009).
12. L. E. Ynoquio Herrera, R. M. Ribeiro, V. B. Jabulka, P. Tovar, and J. Pierre von der Weid, "Photonic generation and transmission of linearly chirped microwave pulses with high TBWP by self-heterodyne technique," *J. Lightwave Technol.* **36**(19), 4408–4415 (2018).
13. W. Li, F. Kong, and J. Yao, "Arbitrary microwave waveform generation based on a tunable optoelectronic oscillator," *J. Lightwave Technol.* **31**(23), 3780–3786 (2013).
14. T. Hao, Q. Cen, Y. Dai, J. Tang, W. Li, J. Yao, N. Zhu, and M. Li, "Breaking the limitation of mode building time in an optoelectronic oscillator," *Nat. Commun.* **9**(1), 1839 (2018).
15. T. Hao, J. Tang, W. Li, N. Zhu, and M. Li, "Harmonically Fourier domain mode-locked optoelectronic oscillator," *IEEE Photonics Technol. Lett.* **31**(6), 427–430 (2019).
16. S. Zhu, X. Fan, B. Xu, W. Sun, M. Li, N. Zhu, and W. Li, "Polarization manipulated Fourier domain mode-locked optoelectronic oscillator," *J. Lightwave Technol.* **38**(19), 5270–5277 (2020).
17. C. Wang and J. Yao, "Chirped microwave pulse generation based on optical spectral shaping and wavelength-to-time mapping using a Sagnac loop mirror incorporating a chirped fiber Bragg grating," *J. Lightwave Technol.* **27**(16), 3336–3341 (2009).
18. M. H. Khan, H. Shen, Y. Xuan, L. Zhao, S. Xiao, D. E. Leaird, A. M. Weiner, and M. J. N. P. Qi, "Ultrabroad-bandwidth arbitrary radiofrequency waveform generation with a silicon photonic chip-based spectral shaper," *Nat. Photonics* **4**(2), 117–122 (2010).
19. Y. Li, A. Rashidinejad, J.-M. Wun, D. E. Leaird, J.-W. Shi, and A. M. Weiner, "Photonic generation of W-band arbitrary waveforms with high time-bandwidth products enabling 39 mm range resolution," *Optica* **1**(6), 446–454 (2014).
20. C. Wang and J. Yao, "Photonic generation of chirped microwave pulses using superimposed chirped fiber Bragg gratings," *IEEE Photonics Technol. Lett.* **20**(11), 882–884 (2008).
21. J. Zhang, O. L. Coutinho, and J. Yao, "A photonic approach to linearly chirped microwave waveform generation with an extended temporal duration," *IEEE Trans. Microwave Theory Tech.* **64**(6), 1947–1953 (2016).
22. L. Zhang, Z. Zeng, Y. Zhang, Z. Zhang, S. Zhang, G. Ni, and Y. Liu, "Frequency-sweep-range-reconfigurable complementary linearly chirped microwave waveform pair generation by using a Fourier domain mode locking optoelectronic oscillator based on stimulated Brillouin scattering," *IEEE Photonics J.* **12**(3), 1–10 (2020).
23. X. Li, S. Zhang, S. Li, J. Chen, and W. Zou, "Generation of tunable linearly chirped signals with long temporal duration in the photonic time-stretched coherent radar," *Opt. Lett.* **45**(20), 5736 (2020).
24. J. Zhang and J. Yao, "Time-stretched sampling of a fast microwave waveform based on the repetitive use of a linearly chirped fiber Bragg grating in a dispersive loop," *Optica* **1**(2), 64 (2014).
25. W. Liu, M. Li, C. Wang, and J. Yao, "Real-time interrogation of a linearly chirped fiber Bragg grating sensor based on chirped pulse compression with improved resolution and signal-to-noise ratio," *J. Lightwave Technol.* **29**(9), 1239–1247 (2011).